Prominent features of deformation and destruction of polycrystalline aluminum

N. V. Zarikovskaya, L. B. Zuev

Institute of Strength Physics and Material Science, Siberian Branch of the Russian Academy of Science, Tomsk, Russia

Tomsk State University of Control System and Radioelectronics, Tomsk, Russia

chepko-znv@mail.ru, lbz@ispms.tsc.ru

Keywords: plastic deformation localization, polycrystalline aluminum, deformation curve, autowave, spatial period, failure

Abstract. The grain size dependence of the wavelength of flow localization observed in the stage of parabolic work hardening of polycrystalline Al has been investigated. The dependence behavior has been defined in the range of grain sizes $8 \cdot 10^{-3} \le D \le 4.5$ mm and the significance of the relationship has been elucidated. The mathematical form of the above dependence has been verified. Geometric method for determination of places of plastic deformation localization has been offered.

Introduction

In the last few years much progress has been achieved toward an understanding of the nature of plastic flow localization by invoking the concept of self-organization of faulted structure. The principal contributions to the comprehension of the problem above were made by Aifantis (1987, 1995,1996) and also by other authors. That the given approach is appreciate and workable is substantiated by the results of the experimental investigations of plastic flow occurring in metals and alloys in a single-crystal and a polycrystalline state (Zuev and Danilov (1999, 2005), Zuev (2001)). It has been found that in the course of this significant and interesting phenomenon, the arrangement and evolution of plastic flow nuclei exhibit certain regular macroscopic features. Thus it is shown that in the stage of linear work hardening ($\sigma \sim \varepsilon$), the flow nuclei form a running wave propagating along specimen extension axis, while in the stage of parabolic work hardening ($\sigma \sim \sqrt{\varepsilon}$), they are arranged into a stationary pattern.

However, to gain a more penetrating insight into the nature of this phenomenon, it is necessary to obtain sufficiently detailed data on the grain size dependence of wavelength observed for polycrystalline materials. By virtue of being a natural structural characteristic, the above quantity is assumed to appreciably affect the parameters of strain localization in the polycrystal. Thus we investigated the space period of flow localization as a function of material grain size as well as the multistage flow behavior.

Experimental conditions

The study was made using 99.85% purity-grade Al specimens. The specimen grain size was tailored in the range of $8 \cdot 10^{-3} \le D \le 4.5$ mm due to recrystallization after preliminary plastic deformation. Grain size was determined by the secant method. In so doing, the variance coefficient of the measured value was about 10%. The specimens having work part 50 × 10 mm were prepared by stamping out of 2 mm-thick Al sheet. These were tested in straining in an "Instron-1185" test machine, the relative straining rate being $\dot{\varepsilon} = 6.7 \cdot 10^{-5}$ s^{-1}. Using the method of speckle interferometry developed by Jones and Wykes (1983), the distribution of plastic distortion tensor components over specimen was determined and the localized strain zones were revealed.

The deforming specimen was photographed in coherent He-Ne laser light. The resulting images of the coherently illuminated specimen surface contained bright spots, the so-called speckles, which were about 3 μm in diameter. The specimen image formed by the photographic lens turned out to be modulated with speckles. When the load was relieved, the specimen was photographed a second time on the same spot of the film, so that another system of speckles shifted with respect to the original one was obtained. The resultant double-exposure speckle interference pattern with two superimposed systems of speckles contained information on the field of the displacement vectors $\boldsymbol{R}(x, y)$ for individual points on the flat specimen. The encoded information was treated by a special optical procedure to reconstruct the $\boldsymbol{R}(x, y)$ field, then the local components of the plastic distortion tensor $\beta = \nabla \boldsymbol{R}(x, y)$, i.e., elongation, ε_{xx}, shear, ε_{xy} and rotation, ω_z, were calculated using numerical differentiation and finally, their distributions over the entire specimen surface or along any specific line, e.g. extension axis, were plotted. Using the above procedure, a set of speckle-modulated images was obtained for the deforming specimen in all the stages of deformation. This permitted step-by-step registration of the variation in the plastic distortion tensor components with growing overall deformation (at a constant straining rate, the total deformation $\varepsilon_{tot} \sim t$). A typical distribution pattern of localized deformation in a tensile specimen is shown in Fig. 1.

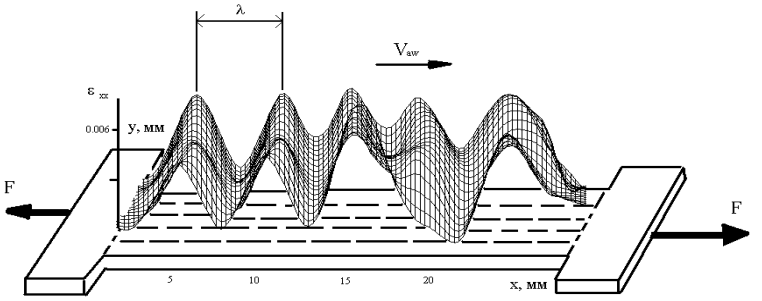

Fig. 1. Phase wave propagating at the stage of linear work hardening

All the tests were performed at the same experimental conditions (shape and size of the specimen, straining rate and temperature), grain size being the only variable.

Multistage behavior of plastic flow in Al polycristals

The use of Al polycrystals furnishes a unique opportunity of checking the validity of the relationship between local strain pattern type and flow curves multi-stage behavior, which was established previously by Zuev and Danilov (1999). It was found by Jaoul (1957) that several stages can be distinguished on the flow curves obtained for Al polycrystals. In this instance, however, the nature and salient features of such multi-stage behavior of the flow curves are different from those of FCC single crystals (see, e.g. Nabarro *et al.* (1964)). Thus all $\sigma(\varepsilon)$ plots show a linear portion, to which corresponds $\sigma = \sigma_1 + \theta\varepsilon$, $\theta = d\sigma/d\varepsilon$ is the coefficient of work hardening; $\sigma_1 = \text{const}$). With growing grain size D, the length of the linear portion becomes less. At $D \geq 0.5$ mm, the above portion of the curve degenerates into a transition point between two stages of parabolic work hardening. In so doing, a jump-wise change occurs in the index $m < 1$

from the expression $\sigma = \sigma_2 + A\varepsilon^m$, which described the latter two stages ($\sigma_2 = \text{const}$). This is in conformity with the finding of Jaoul (1957) that at $T > 77$ K during the deformation of coarse-grain Al and single Al crystals, the stage of linear work hardening is virtually indiscernible on the flow curves obtained.

The investigation of deformation localization in polycrystalline Al, which was carried on by the method of speckle interferometry, has revealed that the localization behavior fully corresponds with the previously established regularities. Thus at the stages of parabolic work hardening a set of stationary localized strain nuclei is found to emerge in the deforming specimen, while at the stage of linear work hardening, an ensemble of equidistant nuclei will propagate synchronously along the specimen at a constant rate, thereby generating a wave process. The change-over of local strain patterns is illustrated in Fig. 2.

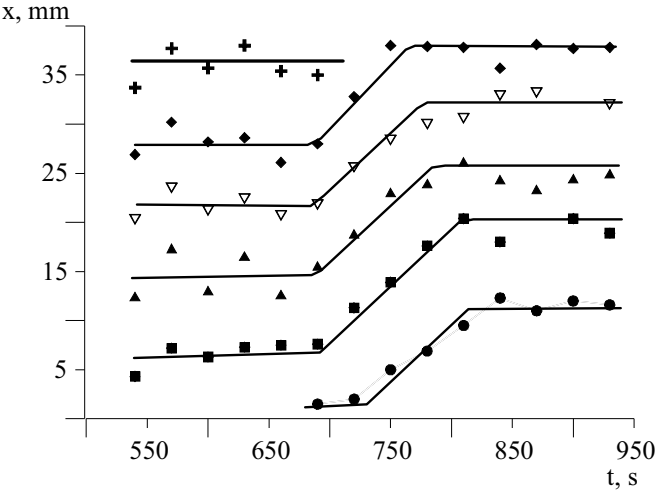

Fig. 2. The kinetics of motion of local strain nuclei during the tensile loading of Al polycrystal (D = 0.2 mm).

As is seen from Fig. 2, the position of the maxima (similar to those in Fig. 1) on the co-ordinates X shift with time. In this case, the inclined portion of the curve corresponds to the stage of linear work hardening (the slope is equal to the rate of propagation of deformation wave) and the horizontal portions to the stages of parabolic work hardening (the rate of propagation is equal to zero).

Wavelength of localized deformation

The experimentally obtained grain size dependence of the space period of strain localization is illustrated in Fig. 3 a, b. From the experimental data it follows that at $D < 0.6$ mm, $\lambda \sim e^D$ (i. e. $\ln\lambda \sim D$, Fig. 3 a), at $0.6 < D < 7$ mm $\lambda \sim \ln D$ (Fig. 3 b) while at $D \geq 10$ mm, λ tends to the limit $\lambda_0 \approx 16$ mm; after the limit is achieved, λ remains virtually the same.

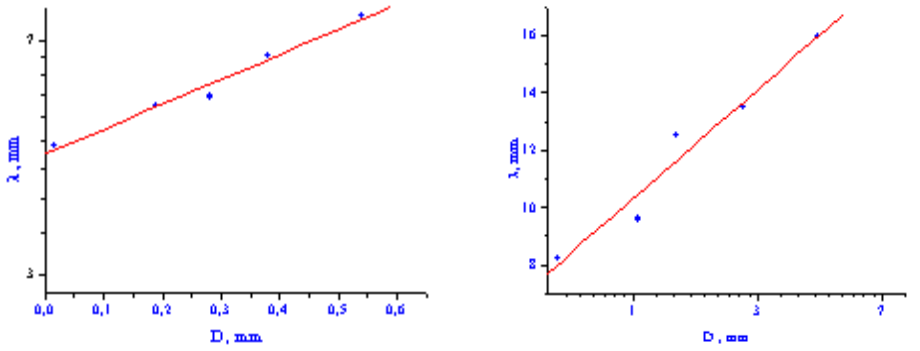

Fig. 3 a, b The grain size D dependence of wavelength λ of localized deformation.
a- region of fine grain, $\lambda \sim e^{D}$;
b- region of coarse grain, $\lambda \sim \ln D$.

Consider the probable nature of the above shape of dependence $\lambda(D)$. It is contended that the relative growth of wavelength $\frac{d\lambda}{dD} \sim \lambda$. However, under the condition that λ becomes commensurable with the specimen size, the relative growth of λ would fall. This is easily taken into account by writing

$$\frac{d\lambda}{dD} = a\lambda - a^{*}\lambda^{2} \tag{1}$$

where a and a^{*} are positive dimensional constants and the square-law term $a^{*}\lambda^{2}$ in the right-hand side of (1) accounts for the reduction in the rate of growth of λ in the range of large D values. Integration of (1) yields the familiar equation of logistic curve (see, e.g., Menzel (1955))

$$\lambda = \frac{\lambda_0}{1 + C \cdot \exp(-aD)}, \tag{2}$$

where $\lambda_0 = a/a^{*}$ and C is the dimensionless integration constant. In order to construct the plot of (2), the co-ordinates $\ln\left(\frac{\lambda_0}{\lambda} - 1\right) - D$ can be conveniently used for straightening of the above curve. The experimental data subjected to the above treatment are presented in Fig. 4. As is seen from Fig. 4, equation (2) describes adequately the set of experimental data, which was obtained for the relation $\lambda(D)$ in a reasonably wide interval of D values.

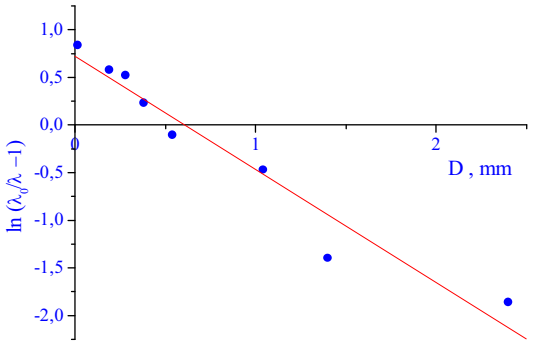

Fig. 4. The reconstruction of the data in Fig. 4 in the co-ordinates $\ln\left(\frac{\lambda_0}{\lambda}-1\right)-D$.

Numerical treatment of the experimental data with the aid of eqn. (2) yields the following values of the constants: a = 1.37 mm^{-1} and a^* = 8.8·10^{-2} mm^2. Correspondingly, λ_0 = 15.6 mm. Zhu *et al.* (1997) and Carsley *et al.* (1997) also investigated the grain size dependence of deformation localization. However, these authors examined alloy in the ultrafine grain range, which hampers comparison of their results with the data presented herein.

In the interval of grain sizes $D \le 0.6$ mm, the term $a^*\lambda^2$ in (1) can be ignored due to it being negligibly small. Then the solution derived from (1) yields the relation $\lambda \sim \exp(aD)$ observed for the above range of D values. On the contrary, in the region of macroscopic D values ($D \ge 1$ mm), over which the rate of growth of λ is found to fall, a relative increase in λ is assumed to be proportional to the number of grains on the specimen work part L_S, i.e.

$$\frac{d\lambda}{dD} \sim L_S/D. \qquad (3)$$

Hence $\lambda \sim \ln D$, as it has been established earlier by Danilov *et al.* (2003) experimentally.

It should be noted that the scale effect (logarithmic dependence of λ on the macroscopic parameter L_S) has been recently established by Zuev (2001) during the investigation of deformation localization in Zr + 2.5% Nb alloy specimens having different length and similar grain size $D \approx 5$ μm. It is found that in the interval $25 \le L_S \le 125$ mm, $\lambda = \lambda^* + \alpha \cdot \ln L_S$ (α and λ^* being constants), i.e. in the range of macroscopic values of D and L_S, the logarithmic type of the dependence between λ and the above variables turns out to be universal enough.

Distinctive features of deformation macrolocalization at the prefracture stage

In order to get a holistic picture of deformation for polycrystalline aluminum, the final stage of the process, i.e. prefracture stage, has been explored. It has been shown earlier that the most striking feature of plastic deformation localization reveals itself at the latter stage.

The prefracture stage is a parabolic one, i.e. the stress-strain dependence for this stage has the form $\sigma \sim \varepsilon^n$ (here n is a parabola exponent). It has been shown that at $n < 0.5$ localized deformation nuclei move along the sample at rate V

$$V(n) = V_0 \cdot (n - q)^2 \,. \qquad (3)$$

At the parabolic stage ($n \approx 0.5$) the localized deformation nuclei become motionless ($V = 0$), while at the linear stage ($n = 1$) they move synchronously at different rates.

The nuclei locations were plotted in $X\ (t)$ or $X\ (\varepsilon)$ coordinates; here X is a nucleus' coordinate; t is deformation time and ε is deformation (Fig. 5).

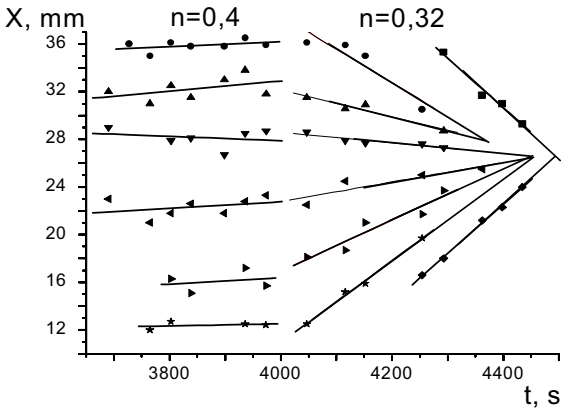

Fig. 5. Positions of localization nuclei v_s time

It can be seen from the plot that at $n \leq 0.4$ the nuclei's trajectories would form a bundle whose pole pinpoints the location of future fracture.

The velocity of a nucleus can be defined from the slope of the straight line. It should also be noted that the nuclei move with different rates, some of them disappearing altogether.

Thus, one can predict the place of future fracture long before the beginning of visible necking.

Model of determination of places of plastic deformation localization by geometric method

It is shown that the plastic waves generated in the various stages of flow have a characteristic macroscopic scale $\lambda \approx 5\ldots10$ mm (Zuev and Danilov (1999), Zuev (2001)), whereas the underlying processes responsible for the material's plasticity occur on the macroscopic scale of order of dislocation ensemble ($\sim 10^{-2}$ mm) (Friedel (1964)).

In order to relate the above two scales, one can use a model based on the following assumptions. Consider the propagation of acoustic impulses emitted, according to, e.g., Gillis and Hamstad (1974), during every elementary plasticity act. As the impulses propagate in the non-uniformly deforming medium, they are likely to be focused at a certain distance from the plastic nucleus acting at the given stage of flow. To do this, the dislocation structure's heterogeneities should be able to act as acoustic lenses. This is quite possible, since the velocity of sound propagation in a medium is found to depend on medium straining (Zuev *et al.* (2003)). Let ξ be the characteristic size (curvature radius) of non-uniformity, then according to Bergman (1954), the focal distance f of such an acoustic lens is given by

$$f \approx \frac{\xi}{n-1}, \qquad (4)$$

where $n = V_0/V$ is the refraction index of acoustic waves (V_0 and V being the rates of ultrasound wave propagation in a deformed and a non-deformed medium, respectively). It is known that by the deformation of Al $n \approx 1.002$ (Zuev *et al.* (2003)) and $\xi \approx 0.01$ mm (for

example, Ball (1957)). Then it follows from (4) $f \approx 5$ mm $\approx \lambda$. It is at this distance that the probability of occurrence of the next shear becomes high. The quantities n and ξ are determined by the material structure; their evolution in the course of plastic flow involves the respective changes in the wave pattern of strain localization.

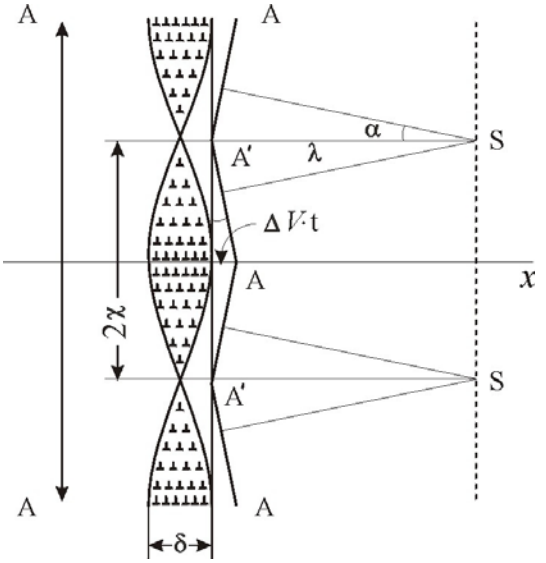

Fig. 6. Geometric determination of places of plastic deformation localization.

Conclusion

We got data that deformation curve of polycrystalline aluminum has multi-stage behavior. On every stages there are localization of plastic deformation. Mathematical form of dependence of macrolocalization on grain size have been gotten. Also we got data about features of plastic deformation localization on the prefracture stage. Geometric method for determination of places of plastic deformation localization has been offered.

References

[1] Aifantis, E.C. (1987) International Journal of Plasticity 3, 211-247.
[2] Aifantis, E.C. (1995) International Journal of Engineering Science 33, 2161-2178.
[3] Aifantis, E.C. (1996) International Journal of Non-Linear Mechanics 31, 797-809.
[4] Friedel, J. (1964) Dislocations. Pergamon Press, London.
[5] Jaoul, B. (1957) Journal of Mechanics and Physics of Solids 5, 95-114 (in French).
[6] Jones, R. and Wykes, C. (1983) Cambridge Univer. Press, Cambridge, London, New York.
[7] Menzel, D. (editor). (1957) Prentice-Hall. Inc., New York.
[8] Nabarro F.R.N., Basinski, Z.S. and Holt, D.B., (1964) Taylor and Francis, London.
[9] Zhu, X.H., Carsley, J.E., Milligan, W.W. and Aifantis, E.C. (1997) Scripta Materialia 36, 727-726.
[10] Zuev, L.B.: Ann. Phys. Vol. 3 (2001), p. 965
[11] Zuev, L.B. Danilov, V.I.: Philosophical Magazine A Vol. 79 (1999), p. 43
[12] Zuev, L.B., Danilov, V.I.: Technical Physics Vol. 50 (2005), p.1636
[13] Zuev, L.B., Semukhin, B.S., Zarikovskaya, N.V.: Int. J. Solids Structure Vol. 40 (2003), p. 941